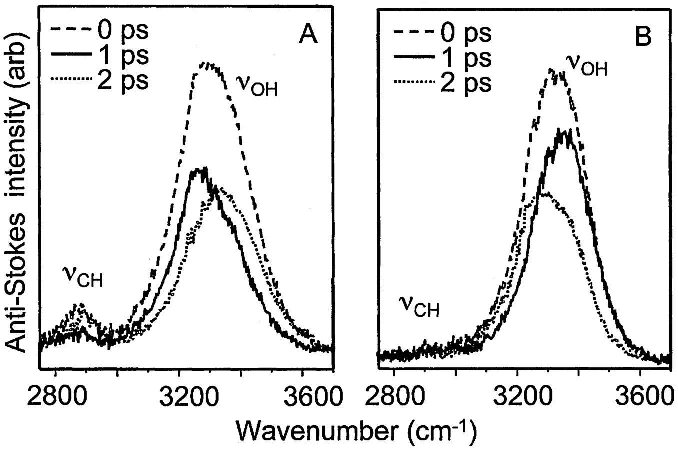

Fig. 4. Transient anti-Stokes spectra after OH stretch pumping, for 1-butanol and *tert*-butanol. (**A**) In 1-butanol, less than 1% of OH stretching excitations are transferred to CH_2 and CH_3 stretching excitations (the Raman cross-section for OH stretching is about 10 times smaller than for CH stretching). (**B**) In *tert*-butanol, no energy transfer is observed from OH to CH stretching. The central carbon atom, which has no CH stretching excitations, chokes off through-bond energy transfer from OH to CH_3.

only about one-third the speed of sound in ethanol (*21*). The overall efficiency for VET from OH to $\nu_a(CH_3)$ states is poor. In ethanol, the instantaneous population of stretching excitations on the terminal CH_3 was never more than about 0.7% of the OH stretch (Fig. 3A), and this efficiency dropped off by about a factor of 2 for each CH_2 added to the chain. That is because at the same time as vibrational energy is moving from OH to CH_3, it is also disappearing into lower energy OH and CH bending and CO stretching vibrations in the 1000 to 1500 cm^{-1} range (*20*), which is not discussed here. Differences in stretching-to-bending transition rates for the different OH, CH, CH_2, and CH_3 groups studied here and the competition between these rates and the rates of intermolecular transfer down the chain account in part for the different absolute vibrational populations of these groups seen in Fig. 3. It would be interesting if we could find other useful vibrational reporter groups with longer lifetimes, such as C≡N (*22*) or aromatic ring-stretching vibrations (*23*), and intervening groups that are better conductors of vibrational energy, so that these studies could be extended to larger molecules and longer distances.

References and Notes

1. G. A. Voth, R. M. Hochstrasser, *J. Phys. Chem.* **100**, 13034 (1996).
2. L. K. Iwaki, J. C. Deàk, S. T. Rhea, D. D. Dlott, in *Ultrafast Infrared and Raman Spectroscopy*, M. D. Fayer, Ed. (Marcel Dekker, New York, 2000).
3. J. C. Deàk, L. K. Iwaki, D. D. Dlott, *Opt. Lett.* **22**, 1796 (1997).
4. E. J. Heilweil, M. P. Casassa, R. R. Cavanagh, J. C. Stephenson, *J. Chem. Phys.* **85**, 5004 (1986).
5. R. Laenen, C. Rauscher, *Chem. Phys. Lett.* **274**, 63 (1997).
6. S. Woutersen, U. Emmerichs, H. J. Bakker, *J. Chem. Phys.* **107**, 1483 (1997).
7. R. Laenen, K. Simeonidis, *Chem. Phys. Lett.* **299**, 589 (1999).
8. R. Laenen, C. Rauscher, A. Laubereau, *J. Phys. Chem. A* **101**, 3201 (1997).
9. T. Förster, *Ann. Phys.* **6**, 55 (1948).
10. V. M. Kenkre, A. Tokmakoff, M. D. Fayer, *J. Chem. Phys.* **101**, 10618 (1994).
11. B. Schrader, *Raman/Infrared Atlas of Organic Compounds* (VCH, Weinheim, Germany, ed. 2, 1989).
12. J.-P. Perchard, M.-L. Josien, *J. Chim. Phys.* (*Paris*) **65**, 1834 (1968).
13. J. C. Deàk, L. K. Iwaki, S. T. Rhea, D. D. Dlott, *J. Raman Spectrosc.* **31**, 263 (2000).
14. X. Hong, S. Chen, D. D. Dlott, *J. Phys. Chem.* **99**, 9102 (1995).
15. S. Woutersen, H. J. Bakker, *Nature* **402**, 507 (1999).
16. A. Nitzan, S. Mukamel, J. Jortner, *J. Chem. Phys.* **63**, 200 (1975).
17. J. S. Hutchinson, W. P. Reinhardt, J. T. Hynes, *J. Chem. Phys.* **79**, 4247 (1983).
18. A. Laubereau, W. Kaiser, *Rev. Mod. Phys.* **50**, 607 (1978).
19. L. K. Iwaki, D. D. Dlott, *Chem. Phys. Lett.* **321**, 419 (2000).
20. ———, *J. Phys. Chem. A* **104**, 9101 (2000).
21. D. R. Lide, Ed., *Handbook of Chemistry and Physics 81st Edition* (CRC, Cleveland, OH, 1996).
22. J. C. Deàk, L. K. Iwaki, D. D. Dlott, *J. Phys. Chem.* **102**, 8193 (1998).
23. L. K. Iwaki, J. C. Deàk, S. T. Rhea, D. D. Dlott, *Chem. Phys. Lett.* **303**, 176 (1999).
24. This material is based on work supported by NSF under award number DMR-0096466, by the Air Force Office of Scientific Research under contract F49620-00-1-0049, and by the Army Research Office contract DAAD19-00-1-0036.

26 February 2002; accepted 24 April 2002

Structure of the 8200-Year Cold Event Revealed by a Speleothem Trace Element Record

James U. L. Baldini,[1]* Frank McDermott,[1] Ian J. Fairchild[2]

Abrupt first-order shifts in strontium and phosphorus concentrations in stalagmite calcite deposited in western Ireland during the 8200-year event (the major cooling episode 8200 years before the present) are interpreted as responses to a drier climate lasting about 37 years. Both shifts are centered on 8330 ± 80 years before the present, coinciding with a large oxygen isotope anomaly and a change in the calcite petrography. In this very high resolution (monthly) record, antipathetic second-order oscillations in phosphorus and strontium reveal decreased growth rates and increased rainfall seasonality. Growth rate variations within the event reveal a two-pronged structure consistent with recent model simulations.

The 8200-year event is widely regarded as the strongest Holocene cooling episode, with clear expressions in Greenland (*1, 2*), the North Atlantic (*3*), Europe (*4–11*), North America (*12–14*), North Africa (*15*), and the Venezuelan Cariaco Basin (*16*). Decreased snow accumulation rates, lower levels of atmospheric methane, and increased atmospheric dust and sea-salt loadings indicate widespread dry conditions (*17, 18*). Explanations usually involve a perturbation of the North Atlantic thermohaline circulation (THC) by increased freshwater inputs associated with the decay of the Laurentide ice sheet (*6, 19*). A high-resolution global circulation model (GCM) indicates that a freshwater pulse of a magnitude similar to that associated with the catastrophic drainage of the large proglacial lakes Agassiz and Ojibway could have produced the 8200-year event, including a very brief warming episode within the event (*20*).

Crucial unresolved questions are whether the cooling occurred as a single event or as a more complex multipulse episode involving partial recovery, and whether the cooling resulted in enhanced seasonality in mid-latitude temperate regions. The latter is important because it may affect the detection of the event by some proxies such as tree rings. The coarse resolution of the available climate records has hampered investigation of these issues. Here, we present a very high resolution trace element record for

---

[1] Department of Geology, University College Dublin, Belfield, Dublin 4, Ireland. [2] School of Earth Sciences and Geography, Keele University, Staffordshire ST5 5BG, UK.

*To whom correspondence should be addressed. E-mail: james.baldini@ucd.ie

the 8200-year event in stalagmite CC3, from Crag Cave in southwestern Ireland (*21*), showing that the event was characterized by rapid deterioration, a brief intra-event amelioration, enhanced seasonality, and an abrupt termination.

Trace elements in carbonate speleothems (stalagmites and stalactites) can provide qualitative proxies for paleo-recharge in well-characterized karst systems (*22–24*). In temperate regions, solute acquisition by karst waters depends on water residence time in the soil and epikarst, and trace element ratios such as Mg/Ca and Sr/Ca tend to increase during drier periods when residence times are longer (*25–27*). Additionally, phosphorus abundances in speleothems frequently exhibit cyclical variations interpreted as annual flushing events from the soil, allowing detailed reconstruction of speleothem growth rates from the spacing between successive annual P peaks (*24*); such data provide an independent proxy for paleo-recharge (*25*).

Approximately 1018 points were analyzed for Mg, Sr, P, Ca, H, and Si at an average spatial resolution of 7.3 μm (*28*) along a 7762-μm track, chosen to traverse a previously documented O isotope shift interpreted to reflect the 8200-year event (*10, 11*). A layer of clear, inclusion-poor calcite 2.5 mm thick occurs within the traverse, coinciding with a sharp increase in Sr and a decrease in P (Fig. 1).[5] Several other clear calcite layers exist within CC3, but systematic sampling reveals no elevated Sr concentrations associated with them, hence the trace element anomalies are not simply the result of variable calcite petrography. Over this "first-order" trace element anomaly, Sr concentrations increase by 89%, from a baseline average of 43 ppm to 81 ppm, accompanied by a 39% decrease in P from an average of 165 ppm to 101 ppm. For the period 10,000 to 5000 years before the present (B.P.), the mean Sr concentration determined by inductively coupled plasma mass spectrometry on drilled calcite is 45 ± 16 ppm, similar to baseline Sr concentrations of 43 ± 7 ppm directly adjacent to the trace element anomaly. On the basis of the published U-Th chronology (*10, 11*), the first-order trace element anomaly commences abruptly at about 8350 ± 80 years B.P., is centered on 8330 ± 80 years B.P., and ends at 8310 ± 80 years B.P. (Fig. 1).

The first-order trace element anomaly (Fig. 1) is synchronous, within the 2σ dating uncertainties, with abrupt shifts in climatic proxies elsewhere indicating the prevalence of cold, dry conditions around 8200 years B.P. (*1, 2, 17, 18*). The anomaly also coincides exactly with the substantial 8 per mil decrease in $\delta^{18}O$ in the same stalagmite, attributed to climatic cooling and a change in the source of vapor supplying rainfall to southwestern Ireland (*10, 11*). The abrupt increase in Sr concentrations centered on 8330 ± 80 years B.P. is interpreted as reflecting an increase in the residence time of water in the glacial till and carbonate bedrock overlying the cave as a result of a drier climate. Although the predominant control on Sr in speleothem calcite is the Sr content of the water (*23*), Sr incorporation also tends to increase with increasing calcite growth rate (*29, 30*). However, the calcite deposited during the first-order shift appears to have resulted from slow, near-equilibrium deposition (*31*), therefore eliminating increased growth rate as an explanation for the elevated Sr concentrations. The synchronous decrease in P is attributed to an overall decline in vegetative cover and rock/till weathering rates due to lower temperatures and decreased precipitation. Nearly all available aqueous phosphorus in soil water is incorporated into plant tissue during the growing season, and previous work indicates that phosphorus is released into groundwater during the autumnal decay of plant matter (*24*). Reduced rock and till weathering rates may have reduced the phosphorus available for vegetative uptake and subsequent autumnal release into the groundwater. The Sr/P ratio is similar before and after the 8200-year event, which suggests that the local hydrologic conditions are similar before and after the event (Fig. 2). However, a change in the parameters controlling the drip water chemistry is indicated by the higher Sr/P ratio of the calcite deposited during the 8200-year event compared with that deposited before and after, suggesting sudden climatic change.

Second-order antipathetic P and Sr oscillations, having wavelengths (λ) typically

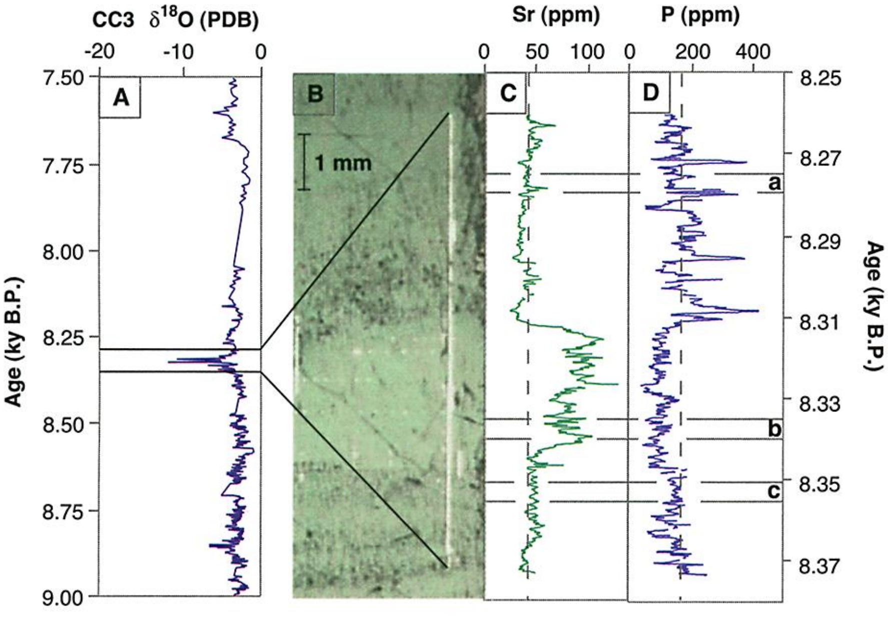

Fig. 1. (**A**) Stalagmite CC3 laser ablation $\delta^{18}O$ record for the period 9000 to 7500 years (9.00 to 7.50 ky) B.P. (*10, 11*). The bracketed area is the interval chosen for ion microprobe analysis. PDB refers to the Pee Dee belemnite standard. (**B**) Photomicrograph of CC3 after analysis, showing principal track. (**C**) CC3 Sr concentration record from 8370 ± 80 years B.P to 8260 ± 80 years B.P. Average Sr values increase markedly from 43 ppm to 81 ppm. (**D**) CC3 P concentration record. Average P values decrease from 165 ppm to 101 ppm. Both first-order trace element excursions are coincident with a lens of clear calcite. These anomalies are synchronous with a previously documented O isotope excursion within CC3, interpreted as reflecting the 8200-year event (*10, 11*). Dashed lines in (C) and (D) represent the mean trace element values for the baseline outside of the event. Letters a, b, and c correspond to intervals expanded in Fig. 3.

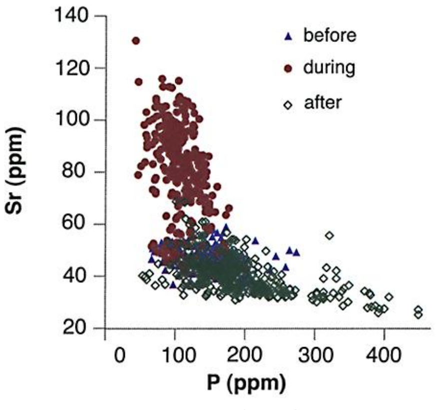

Fig. 2. Sr concentrations plotted against P concentrations. The slope of the line describing the points before (slope = −0.05) and after (slope = −0.06) is nearly identical and is significantly different from that during the event (slope = −0.33). The different relationships between Sr and P during and outside of the event indicate the existence of a different set of parameters controlling the geochemistry of the drip waters. Similar slopes before and after the first-order anomaly indicate a return to baseline conditions, eliminating the possibility that the trace element anomaly was caused by a permanent shift in the local hydrology unrelated to climate.

around 75 μm, are apparent during and preceding the first-order trace element anomaly (Fig. 3, A and B) but are discontinuous after the anomaly (Fig. 3C). Identical antipathetic relationships between P and Sr were identified previously in stalagmites from strongly seasonal climates (*26*) and were attributed to seasonal changes in the concentration of these elements in the infiltrating drip waters. P maxima and Sr minima probably occur during periods of increased infiltration in the autumn (*24, 26*), and Sr maxima may result from drier summer weather (*23*). The second-order trace element oscillations represent annual cycles of calcite deposition, as in other stalagmites (*22, 24, 32, 33*). The amplitude of the Sr oscillations during the first-order anomaly is four times that of the oscillations preceding the anomaly (Fig. 3); this finding suggests increased seasonality in effective precipitation, perhaps due to drier summers. However, no accompanying statistical change in the amplitude of the P cycles is evident (*34*), which suggests that the 8200-year event was either too brief or too mild to alter the seasonal phosphorus cycle.

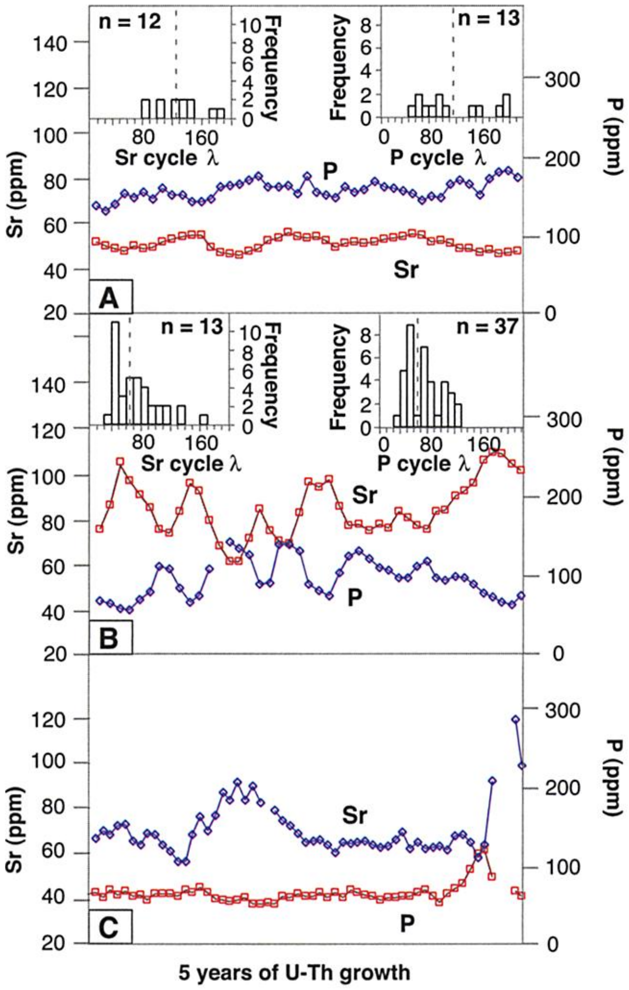

Fig. 3. (**A**) Very well defined second-order antipathetic cycles (mean λ_{Sr} = 120.9 μm; mean λ_P = 117.0 μm, inset) occurring before the 8200-year event, representing annual deposition of calcite. (**B**) Some of the antipathetic cycles (mean λ_{Sr} = 64.7 μm; mean λ_P = 65.8 μm, inset) within the 8200-year event. The λ_{Sr} and λ_P are lower than those preceding the event, suggesting a decrease in annual growth rates caused by a drier climate and colder temperatures. The amplitude of the Sr cycles increases markedly (from 4.2 ppm before to 18.2 ppm during the event), suggesting enhanced seasonality in rainfall. (**C**) Second-order trace element variations after the event. No cyclicity is present, suggesting decreased seasonality in rainfall. Recently deposited calcite from the top of CC3 is also devoid of annual cyclicity, reflecting the modern maritime climate. The locations of these three panels on the complete trace element record are shown at a, b, and c in Fig. 1.

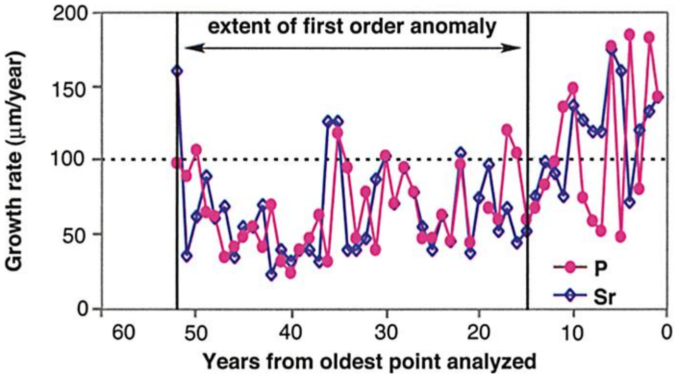

Fig. 4. Annual axial calcite deposition rates for stalagmite CC3 reconstructed using the wavelengths of annual Sr and P cycles. The bracketed area indicates the timing of the 8200-year event, as assessed from the first-order trace element shifts. The horizontal dashed line represents the approximate growth rate of stalagmites in temperate regions. Growth rates decrease into the event, increase briefly 27 years into the event, then increase until the termination of the event. Thirty-eight Sr cycles and 37 P cycles exist within the 8200-year event, suggesting that the hydrologic response to the event lasted about 37.5 years. Trace element cyclicity was nonexistent after the event, precluding cycle counting.

Reconstruction of stalagmite growth rate changes is possible because trace element cycle wavelength is equivalent to the amount of stalagmite calcite deposited in 1 year. The mean wavelengths of Sr and P cycles during the event (Fig. 3B) are approximately half those associated with the period before the event (Fig. 3A); this result suggests reduced growth rates within the event, consistent with reduced rainfall (*25*) and reduced mean annual temperatures (*35*).

Estimates of the duration of the 8200-year event are possible by counting the second-order annual trace element cycles within the first-order anomaly (Fig. 4). Thirty-eight Sr cycles and 37 P cycles, independently counted, exist within the portion of the record defined by the first-order trace element excursion. Hence, the hydrologic response to the 8200-year event lasted about 37.5 years in western Ireland. Annual growth rates preceding the 8200-year event, reconstructed with the use of four collinear U-Th–dated points (*10, 11*), are similar to growth rates before the event (as assessed from the measured wavelengths of the Sr and P cycles), indicating that the cycles are annual. A decrease in annual growth rates is apparent at the inception of the event but gives way to a sudden, short-lived growth increase (Fig. 4). Growth rates decrease again and eventually increase gradually toward the termination of the event. A two-pronged structure is also evident in coarser resolution records of the 8200-year event, including CC3 $\delta^{18}O$ data (*10, 11*), Greenland Ice Sheet Project 2 accumulation rate (*36*) and $\delta^{18}O$ (*2, 37*) data, and numerous Norwegian lacustrine sediment cores (*9*). The overall decrease in growth rate is consistent with cold, dry conditions, because growth rate is predominantly dependent on surface temperature and the amount of precipitation (*35, 38, 39*).

The rapid commencement of the first-order trace element excursion suggests a single catastrophic triggering event, potentially the draining of glacial lakes Agassiz and Ojibway through the St. Lawrence and into the North Atlantic (*19*). It is noteworthy that a GCM modeled response to a freshwater pulse equivalent to the volume of water drained from Lakes Agassiz and Ojibway, 4.67 × 10^{14} m^3, distributed into the Labrador Sea over 20 years, predicts a two-pronged event similar to the trace element record (*20*). This implies a mean meltwater flux of 0.75 Sv (1 Sv = 10^6 m^3 s^{-1}), easily exceeding that required to trigger a collapse of the THC (*40*). The short duration of the event compared with that of high-latitude ice cores may reflect a nonlinear threshold response in atmospheric circulation patterns or in the hydrologic system at this maritime mid-latitude site. The rapid return to baseline trace element values in stalagmite CC3 at 8310 ± 80 years B.P. is consistent with a rapid reestablishment of North Atlantic THC (*20*) ending the cold, dry episode in Ireland.

References and Notes

1. W. Dansgaard *et al.*, *Nature* **364**, 218 (1993).

→ P. M. Grootes, M. Stuiver, J. W. C. White, S. J. Johnsen, J. Jouzel, *Nature* **366**, 552 (1993).

3. G. Bond *et al.*, *Science* **278**, 1257 (1997).
4. D. Klitgaard-Kristensen, H. P. Sejrup, H. Haflidason, S. Johnsen, M. Spurk, *J. Quat. Sci.* **13**, 165 (1998).
5. D. R. Rousseau, R. Precce, N. Limondin-Lozouet, *Geology* **26**, 651 (1998).
6. U. von Grafenstein, H. Erlenkeuser, J. Muller, J. Jouzel, S. Johnsen, *Clim. Dyn.* **14**, 73 (1998).
7. U. von Grafenstein, H. Erlenkeuser, A. Brauer, J. Jouzel, S. J. Johnsen, *Science* **284**, 1654 (1999).
8. A. Korhola, J. Weckstrom, *Quat. Res.* **54**, 284 (2000).
9. A. Nesje, S. O. Dahl, *J. Quat. Sci.* **16**, 155 (2001).
10. F. McDermott, D. P. Mattey, C. Hawkesworth, *Science* **294**, 1328 (2001).
11. For U-Th data [supplement to (*10*)], see www.sciencemag.org/cgi/content/full/294/5545/1328/DC1.
12. I. D. Campbell, C. Campbell, M. J. Apps, N. W. Rutter, A. B. G. Bush, *Geology* **26**, 471 (1998).
13. W. E. Dean, *Geol. Soc. Am. Spec. Pap. 276*, 135 (1993).
14. F. S. Hu, H. E. Wright, E. Ito, K. Lease, *Nature* **400**, 437 (1999).
15. F. A. Street-Perrott, R. A. Perrott, *Nature* **358**, 607 (1990).
16. K. Hugen, J. T. Overpeck, L. C. Peterson, S. Trumbore, *Nature* **380**, 51 (1996).
17. R. B. Alley *et al.*, *Geology* **25**, 483 (1997).
18. T. Blunier, J. Chappellaz, J. Schwander, B. Stauffer, D. Raynaud, *Nature* **274**, 46 (1995).

→ D. C. Barber *et al.*, *Nature* **400**, 344 (1999).

20. H. Renssen, H. Goosse, T. Fichefet, J.-M. Campin, *Geophys. Res. Lett.* **28**, 1567 (2001).
21. Stalagmite CC3 was chosen because of its location on the North Atlantic margin and because previous work detected the 8200-year event as the only high-amplitude O isotope excursion during the entire Holocene (*10, 11*).
22. M. S. Roberts, P. L. Smart, A. Baker, *Earth Planet. Sci. Lett.* **154**, 237 (1998).
23. I. J. Fairchild *et al.*, *Chem. Geol.* **166**, 255 (2000).
24. I. J. Fairchild *et al.*, *J. Geol. Soc.* **158**, 831 (2001).
25. D. Genty, Y. Quinif, *J. Sediment. Res.* **66**, 275 (1996).
26. Y. Huang *et al.*, *Chem. Geol.* **175**, 429 (2001).
27. J. Mayer, *J. Cave Karst Stud.* **61**, 131 (1999).
28. Elemental concentrations were analyzed with a CAMECA ims-4f ion microprobe at the Department of Geology and Geophysics, University of Edinburgh. The primary ion beam excavates pits to a depth of 2 to 5 μm (*41*). Each analyzed spot (diameter 10 μm) was ablated for 15 s before data acquisition to eliminate surface contamination. Si was used to monitor silicate detritus, and data points with Si concentrations greater than 60 ppm and trace element concentrations more than 15% above a 19-point moving average baseline were excluded. Because the bedrock above Crag Cave is a rather pure limestone, Mg does not exhibit any structure and is therefore not discussed. The factors controlling H are poorly understood, and it exhibits no systematic trends. The age of the calcite at the beginning and end of the 7762-μm track, determined by linear interpolation between U-Th–dated points (*10, 11*), corresponds to 8260 ± 80 years B.P. and 8370 ± 80 years B.P., respectively. Several shorter ancillary tracks parallel to and overlapping the principal track (Fig. 1) confirmed the reproducibility of data. The principal track consists of 1018 data points, corresponding to an actual mean spacing of 7.3 μm, implying an average spot overlap of 27%.
29. R. B. Lorens, *Geochim. Cosmochim. Acta* **45**, 553 (1981).
30. Y. Huang, I. J. Fairchild, *Geochim. Cosmochim. Acta* **65**, 46 (2001).
31. Slow, near-equilibrium calcite deposition typically results in optically clear calcite with few inclusions, which is characteristic of the calcite deposited during the first-order shift. A simultaneous decrease in inferred U-Th growth rates (*10, 11*) and growth rates reconstructed by counting trace element cycles within the calcite (discussed in the text) corroborates the contention that the clear calcite within the event was the result of slow, near-equilibrium deposition.
32. A. Ayalon, M. Bar-Matthews, A. Kaufman, *The Holocene* **9**, 715 (1999).
33. A. A. Finch, P. A. Shaw, G. P. Weedon, K. Holmgren, *Earth Planet. Sci. Lett.* **186**, 255 (2001).
34. Mean amplitude was quantified by calculating the standard deviation of the detrended subsets (before, during, and after the event) of the data.
35. D. Genty, A. Baker, B. Vokal, *Chem. Geol.* **176**, 191 (2001).

→ R. B. Alley *et al.*, *Nature* **362**, 527 (1993).

→ M. Stuiver, P. M. Grootes, T. F. Braziunas, *Quat. Res.* **44**, 341 (1995).

38. A. Baker, P. L. Smart, D. C. Ford, *Palaeogeogr. Palaeoclimatol. Palaeoecol.* **100**, 291 (1993).
39. D. Genty, Y. Quinif, *J. Sediment. Geol.* **66**, 275 (1996).
40. A. Schmittner, M. Yoshimori, A. J. Weaver, *Science* **295**, 1489 (2002).
41. R. W. Hinton, in *Microprobe Techniques in the Earth Sciences*, P. J. Potts, J. F. W. Bowles, S. J. B, Reed, M. R. Cave, Eds. (Chapman, London, 1995), pp. 235–289.

42. We gratefully acknowledge the assistance of R. Hinton and J. Craven with the ion microprobe at the University of Edinburgh. We thank the owners of Crag Cave for their continued cooperation and enthusiasm. We thank two anonymous reviewers for their constructive reviews. Supported by Enterprise Ireland grant SC/1999/012/.

12 March 2002; accepted 1 May 2002

Insights into Collisional Magmatism from Isotopic Fingerprints of Melting Reactions

Kurt M. Knesel[1]* and Jon P. Davidson[2]

Piston-cylinder experiments in the granite system demonstrate that a variety of isotopically distinct melts can arise from progressive melting of a single source. The relation between the isotopic composition of Sr and the stoichiometry of the observed melting reactions suggests that isotopic signatures of anatectic magmas can be used to infer melting reactions in natural systems. Our results also indicate that distinct episodes of dehydration and fluid-fluxed melting of a single, metapelitic source region may have contributed to the bimodal geochemistry of crustally derived leucogranites of the Himalayan orogen.

The isotopic characteristics of melt and restite during anatexis have not been studied in detail in controlled laboratory experiments. It is assumed that the isotopic compositions of melts are given by the bulk composition of the protolith—an assumption that implies isotopic equilibration is attained between the melt and source minerals. Recent observations have called this assumption into question at shallow crustal pressures (*1–3*), leading us to extend the question to deeper levels in the crust. Here we report experimental results on dehydration melting involving both muscovite and biotite and show how the results can be used to infer melting reactions involved in the petrogenesis of crustally derived granites of the Himalayan orogen. Such information is useful for understanding the role of fluids and the influence of deformation on anatectic melting during collisional orogenesis.

Experiments were performed at 600 MPa and 850 to 1000°C in a piston-cylinder apparatus with the use of a diamond-aggregate extraction technique (*4*). In a melt-extraction experiment, a thin layer of ~50-μm-sized diamonds is loaded on top of ~300 mg of 75- to 100-μm-sized grains of crushed granite in a graphite cylinder housed in a large-volume, thick-walled Ni capsule (*5*). The use of crushed granite rather than a fine powder or gel is a unique and important aspect of the experimental design because it allows us to simulate the influence of minerals on isotopic variations during melting. When brought to run conditions (*6*), partial melt from the crushed granite is driven into pore space in the overlying diamond powder by the transient pressure gradient between the two layers. At the end of the experiment, quenched melt (glass) in the diamond layer is separated from the residual silicate (crushed granite) by sectioning with a diamond wafer saw. The glass is dissolved away from the diamond, and the Sr-isotopic compositions in the glass are measured by thermal ionization mass spectrometry (*7*).

Variation of $^{87}\mathrm{Sr}/^{86}\mathrm{Sr}$ ratios of experimental melts as a function of the duration of the experiment shows that, for short durations, the isotopic composition of the melt is distinct from that of the bulk starting assemblage (Fig. 1). However, the $^{87}\mathrm{Sr}/^{86}\mathrm{Sr}$ of the melt approaches that of

---

[1] Department of Earth Sciences, University of Queensland, Brisbane, Qld 4072, Australia. [2] Department of Earth Sciences, University of Durham, Durham, DH1 3LE, UK.

*To whom correspondence should be addressed. E-mail: k.knesel@earth.uq.edu.au